Journal of Genetics (2024)103:16
https://doi.org/10.1007/s12041-024-01466-w

RESEARCH ARTICLE

Genetic characterization and linkage analysis of spotted leaf 6, liguleless and lax panicle traits in mutant rice

MOHAMMAD NURUL MATIN[1,2], KYUNG EUN LEE[3] and SANG GU KANG[1]*

[1]*Department of Biotechnology, Institute of Biotechnology, College of Life and Applied Sciences, Yeungnam University, Gyeongsan 38541, Republic of Korea*
[2]*Molecular Genetics Laboratory, Department of Genetic Engineering and Biotechnology, University of Rajshahi, Rajshahi 6205, Bangladesh*
[3]*Sunforce Inc, 208-31, Gumchang-ro, Yeungcheon-si, Gyeongsangbuk-do 31882, Republic of Korea*
*For correspondence. E-mail: kangsg@ynu.ac.kr.

Received 14 October 2023; revised 16 January 2024; accepted 24 January 2024

Abstract. Phenotypic mutants are valuable resources for elucidating the function of genes responsible for their expression. This study examined mutant rice strains expressing three traits: spotted leaf 6 (*spl6*), lax panicle (*lax*), and liguleless (*lg*). In the mutant, the *spl6* phenotype was a genetically programmed lesion-mimicking mutation (LMM) that displayed spontaneously scattered spots across the leaf surface. In the *lg* trait, the plant lacked a collar region, and there were no auricles and ligules at the junction of the leaf blade and leaf sheath. The *lax* panicle trait manifested as sparely arranged spikelets resulting from the terminal spikelet with no lateral spikelets, which caused a drastic reduction of the total seed number in the mutant. All three mutant genes were genetically recessive and had nuclear gene regulation. The dihybrid segregation of the *lg* gene was classified independently according to the Mendelian 9:3:3:1 dihybrid segregation ratio in the F_2 generation, suggesting that the *lg* gene is not linked to the same chromosome as the *lax* and *spl6* genes. On the other hand, *spl6* and *lax* were not assorted independently, indicating that they are closely linked on chromosome 1 in rice. Additional linkage analysis from the recombination of *spl6* and *lax* genes reconfirmed that the two genes were ~9.4 cM away from each other. The individual single-gene mutant plant from one plant with a three-gene mutation (*spl6, lax*, and *lg*) was isolated and characterized, which will be a crucial resource for the gene cloning and molecular characterization of these genes.

Keywords. lesions mimic mutant; program cell death; spotted leaf; liguleless; lax panicle; *Oryza sativa*.

Introduction

Genetic analysis of mutations provides a powerful tool to reveal complex processes of plant growth and development. Mutants are valuable resources that could provide genetic loci to generate improved crops. This study evaluated a rice mutant with various phenotypic expressions at the vegetative and reproductive stages, displaying lesion mimic mutant (LMM) spotted leaf 6 (*spl6*), liguleless (*lg*), and lax panicle (*lax*) mutant phenotypes according to phenotypic and genetic analyses.

LMM plants develop scattered dotted spots throughout leaf surfaces without stress from pathogenic infection. On the other hand, a genetically regulated signalling pathway leads to death of the localized cell, known as programmed cell death (PCD) (Balagué *et al.* 2003; Zeng *et al.* 2004; Matin *et al.* 2006; Mori *et al.* 2007; Williams and Dickman 2008; Bruggeman *et al.* 2015; Xia *et al.* 2019; Kang *et al.* 2021; Zheng *et al.* 2022; Zhao *et al.* 2023). Various stress elicitors, such as biotic and abiotic stresses, mechanical damage from temperature, light, wind, as well as reactive oxygen species (ROS), have been identified as influential for the PCD and lesion development in plants (Takahashi *et al.* 1999; Balagué *et al.* 2003; Matin *et al.* 2006; Kang *et al.* 2021; Wu *et al.* 2023). Thus far, more than 30 LMM in rice, including several LMMs in many other plants, have been studied intensively for their genetic mechanism, underscoring the importance of further research using this mutant (Yamanouchi *et al.* 2002; Wang *et al.* 2005, 2019; Ma *et al.* 2019; Ruan *et al.* 2019; Liu *et al.* 2021; Yuchun *et al.* 2021; Chen *et al.* 2022; Li *et al.* 2022; Shang *et al.* 2022; Wu *et al.* 2023). Recent extensive reviews described that most LMMs

Published online: 17 April 2024

have been identified in rice and other plants (Kang *et al.* 2021; Yan *et al.* 2022). The present study analysed the *spl6* mutant, which forms tiny dotted lesions at the early tillering stage in leaf and gradually increase in size.

Morphologically, the rice leaf is structured with a leaf sheath and leaf blade with a laminar joint between them called the collar, surrounded by two hairy sickle-shaped auricles and a tongue-like white apparatus called the ligule. These specialized organs help to keep the leaf sheath and culm together and prevent dust entry. The collar helps to bend the leaf to facilitate photosynthesis (Hoshikawa 1989; Lee *et al.* 2007b). In the *lg* phenotype, the leaf sheath is connected directly to the leaf blades without a collar region. Therefore, the ligule and auricle of *lg* are not formed resulting in upright and high erectness of leaf. Similarly, rice *lg* mutant, *OsLG1*, have been identified to lack all the three organs (Lee *et al.* 2007b).

In rice, the panicle density is regarded as the most important characteristic from a breeding point of view because it is closely associated with the grain yield. Rice panicles develop at the reproductive stage of the plant development by phase transition of the shoot apical meristem. After the transition, the inflorescence meristem produces primary branch meristems that develop a primary panicle branch. The primary panicle branch also produces secondary branch meristems that produce secondary panicle branches or differentiate into lateral spikelets. Finally, both meristems differentiate into a terminal spikelet (Yamagishi *et al.* 2004; Oikawa and Kyozuka 2009). Thus, the pattern of apical meristem formation has particular significance in crop spikelets development.

In contrast, the *lax* panicle mutant is characterized by a few elongated rachis branches and reduced spikelets on the panicle. Rice *LAX PANICLE1* (*LAX1*) is required to generate the branch meristem. Hence, the *lax1* mutant fails to form a branch meristem, leading to reduced spikelets (Oikawa and Kyozuka 2009; Matin and Kang 2012). The rice panicle starts via the limited growth of inflorescence consisting of primary branches, secondary branches, and spikelets on the branches. The panicle architecture affects the grain number per panicle and grain yield. Therefore, apical meristem formation and panicle structure development have attracted considerable interest for improving rice quality since they contribute directly to crop yield.

Although several phenotypic mutations have been identified so far, more intensive research on materials with clear specific phenotypic expression is needed to identify the function and regulatory mechanism of specific mutations in rice. From various individual studies, the *spl6*, *lg*, and *lax* genes were identified as recessive genetically controlled compared to the normal genes (Mori *et al.* 1973; Lee *et al.* 2007a,b; Matin and Kang 2012; Kang *et al.* 2021). On the other hand, a few studies have examined the linkage and genetic correlation of these three genes in rice. The present study used a mutant rice plant with homozygous recessive genes for these three genetic traits, and their Mendelian genetic relationships were revealed. These findings may provide fundamental information about the molecular functions of these genes in the future.

Materials and methods

Plant materials and phenotype analysis

Rice YUM111 (FL269 lines) mutant (*O. sativa* Japonica type) is one of the mutant lines induced by N-methyl-N-nitrosourea (MNU) that was derived at Kyushu University, Japan (Kumamaru *et al.* 1988). The mutant exhibited distinct spots on leaves, liguleless, and lax-type panicle phenotypes. Rice plants were grown under natural conditions between 30 and 35°C in the research field of Yeungnam University, Gyeongsan, Republic of Korea, and the phenotypic characteristics were documented. The observed characteristics were as follows: spot formation time, colour, shape, size, and arrangement of spots; the severity of spots at different developmental stages; presence and absence of a collar, auricle, and ligule at the leaf junction; panicle structure; length and spikelet formation type; number of primary rachis branches and secondary rachis branches; number of nodes per rachis branch; and number of spikelets.

Genetic analysis

For inheritance analysis, the mutant line was hybridized to wild-type pollen donors IRRI347 (YUC084) (*O. sativa* Indica type) and Donghechal (YUC005) (*O. sativa* Japonica type). The F_1 plants were grown and self-fertilized to produce the F_2 progeny. The phenotypic data of the F_2 plants were documented throughout the developmental stages for the concerned genes. The genotype of individual F_2 plants was detected from their segregating feature in the F_3 progeny. The genotype of the plants was confirmed by planting 20 seeds of each dominant F_2 plant in the field and determining the heterozygous plants. The phenotypic data were collected from the F_3 plants, and their homozygosity and heterozygosity were detected based on their segregation. Phenotypic data were collected from 558 F_3 plants. Segregation of individual gene for the monohybrid cross was evaluated based on the Mendelian 1:3 phenotypic ratios. Dihybrid crosses for the co-segregation of two genes were evaluated based on the Mendelian 9:3:3:1 phenotypic ratio. By considering crosses between the *lax* and *spl6* genes, parental and recombinant plants were calculated, and their distance was measured in centimorgans (cM).

Results and discussion

Phenotype of the spl6 mutation

The *spl6* mutant line formed spontaneous lesions on the leaf blades (Matin *et al.* 2006; Kang *et al.* 2007). The phenotypic observation indicated that no visible spots were initiated at the early stage. On the other hand, a tiny appearance occurred at the tillering stage. The lesions progressed intensively throughout the leaf surface parallel to the leaf minor vain and rarely on major vain, which was visible at the milk stage. New spots continued to appear until maturity. Lesion formation was diffused, with lesions starting sparsely and rapidly expanding over the entire leaf blade, becoming denser toward the apex and thinner toward the leaf base (figure 1).

Interestingly, flag leaves of the mutant were more heavily spotted than the other leaves. The sunlight intensity significantly affects leaf lesion formation, development, and acceleration in the mutant plants, indicating that lesion formation in the LMMs may be linked directly to the light reactions of the photosynthesis process (Yamanouchi *et al.* 2002; Zeng *et al.* 2004; Qiu *et al.* 2019; Zhang *et al.* 2019; Yao *et al.* 2021; Jiang *et al.* 2022). Moreover, the pattern of spot formation was the progressive type with the developmental stages, which is similar to those in *spl3, spl4*, and *spl7* mutant rice (Yamanouchi *et al.* 2002; Matin *et al.* 2006; Kang *et al.* 2021).

Phenotype of the lg mutation

The leaves of normal rice are composed of a leaf blade and a leaf sheath separated by a laminar joint. Between the leaf blade and leaf sheath, a white band-type laminar joint, called a collar, is present from where two horn or sickle-like auricles and tongue-like ligules are overextended. The lamina joint organ connects the leaf blade to the sheath and causes the leaf blade to bend away from the vertical axis known as the leaf angle, affecting light capture in rice. Thus, this structure is a key factor for the crop yield (Liu *et al.* 2019; Tian *et al.* 2019; Wang *et al.* 2021; Qin *et al.* 2023). On the other hand, a lamina joint-like collar did not exist in the YUM111 mutant. Therefore, the ligule and auricle were also not projected, resulting in a direct assembly of the leaf blade and sheath without vertical bending. In the wild type, the leaf blade forms a long angle with the stem, whereas the mutant ligule-less leaf is erect and forms a small angle with the stem (figure 1).

Plant architecture-related genes are the critical regulators of plant growth, development, and yield (Qin *et al.* 2023).

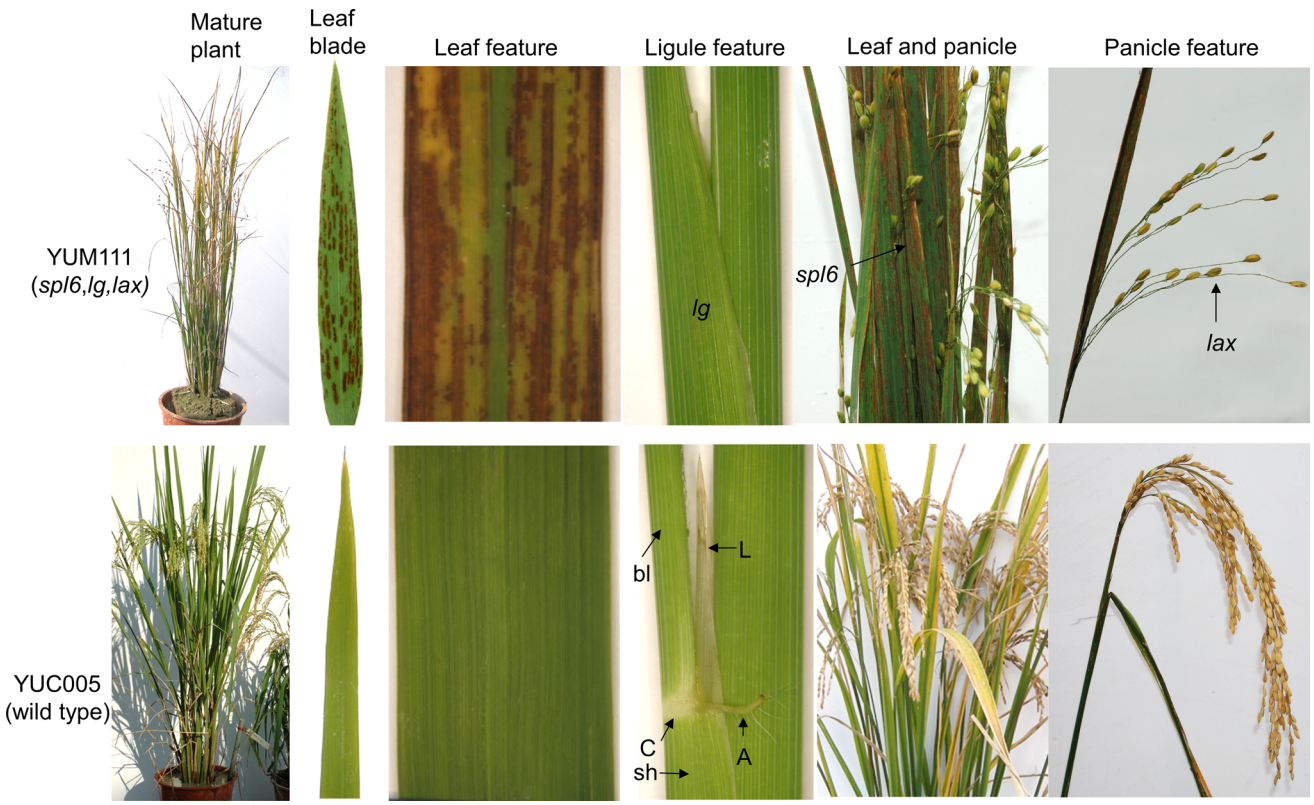

Figure 1. Phenotypes of the wild type (YUC005) and mutant (YUM111) plants for the *spl6*, *lg*, and *lax* mutations. In the mutant parent, for *spl6*, severely spotted matured flag leaf and magnified leaf segment; for *lg*, liguleless phenotype with no collar, auricle, and ligules at the leaf blade and leaf sheath junction; for *lax*, plant upper part and an individual panicle are demonstrated. The corresponding phenotypes of the wild-type plant are also indicated for comparison. L, ligules; C, collar; A, auricles; bl, leaf blade; sh, leaf sheath.

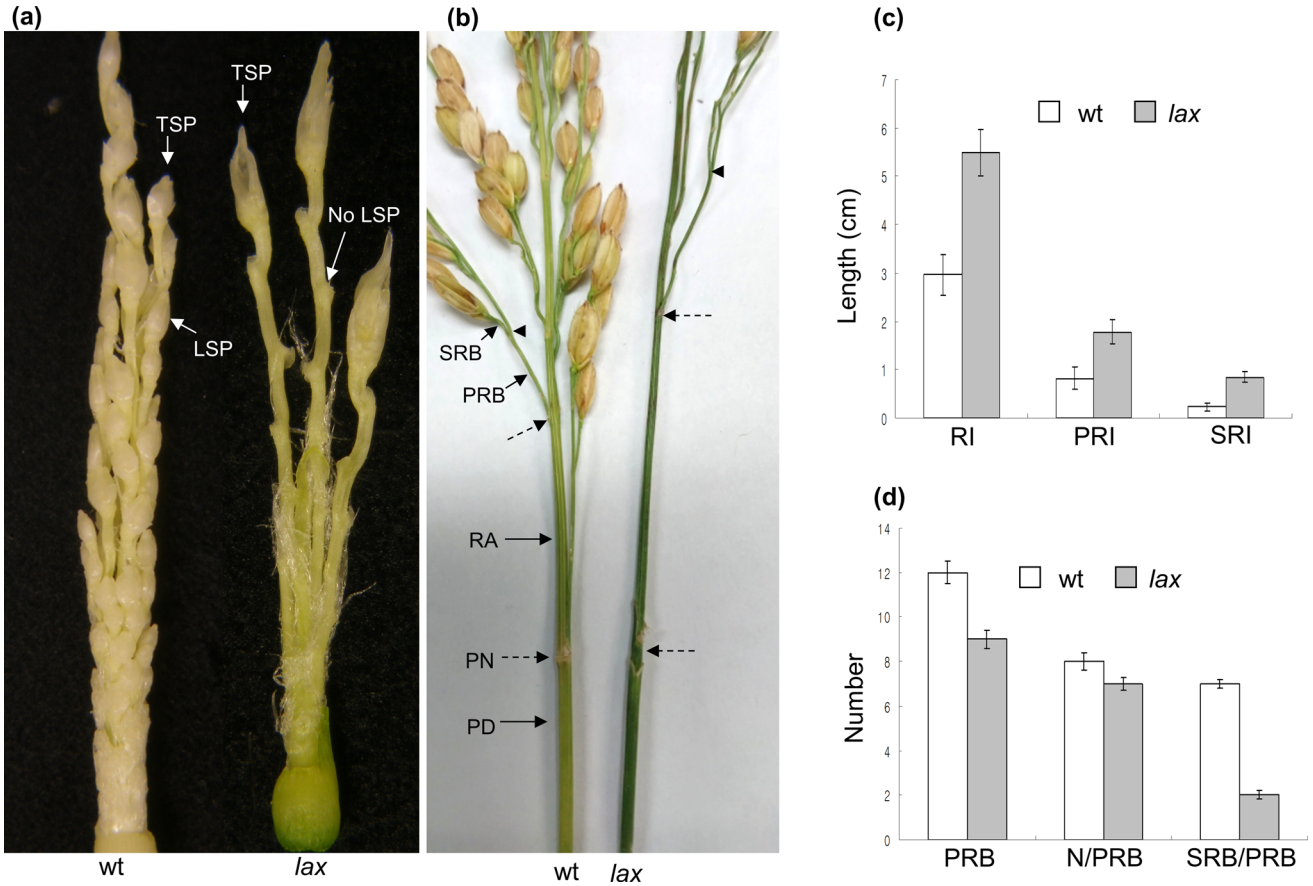

Figure 2. Panicle phenotypic differences between the wild type and *lax.* (a) Developing inflorescence of the rice. The terminal spikelet (TSP) and lateral spikelets (LSP) developed in the primary and secondary rachis branch nodes of the wild type. Only TSP comes from the rachis branches nodes, being empty at the following node in the mutant. (b) Portion of the panicle at the mature stage. PD, peduncle; PN, panicle node; RA, rachis; PRB, primary rachis branch; SRB, secondary rachis branch. The dashed arrows indicate the rachis nodes and the length of the internode. The arrowheads indicate the primary rachis branch nodes. (c) Length (cm) of rachis internode (RI), primary rachis internode (PRI), and secondary rachis internode (SRI) of wild type (wt) and mutant (*lax*). (d) The total number of primary rachis branches (PRB) per panicle, number of nodes per primary rachis branch (N/PRB), and number of secondary rachis branches per primary rachis branch (SRB/PRB). The standard errors are from an average of five individual counts.

One of the related genes, *liguleless* (*lg*), is exclusively a key regulator of the leaf angle and flower development. Some other similar types of rice mutants that resembled the present mutant include the following: *auricleless* (*aur*), which lacks the auricle and ligule; *liguleless* (*lg*) with a defective ligule, auricle, and collar (Maekawa 1988); and *collarless* (*col*), which lacks the collar region (Sanchez 1998). Identifying relationships with leaf angle genes may help control the plant phenotypes to increase yields. Including the present genotype, most of the identified *lg* mutant genotypes showed erect leaves that can maximize the use of light, allow light to pass to the lower canopy, and achieved a higher yield (Wang *et al.* 2020, 2021; Qin *et al.* 2023).

Phenotype of the lax mutation

The rice panicle develops during the reproductive stage via a phase transition of the shoot apical meristem to inflorescence primordia initiation. Rice inflorescence is repeatedly branched to form primary and secondary rachis branches on the panicle axis that develop individual florets on the rachis branches and terminates in a spikelet on both primary and secondary branches that determine the panicle structure (Yamagishi *et al.* 2004; Bell and Bryan 2008; Yoshida *et al.* 2012). Dysfunction of regulatory genes at any stage of inflorescence development can result in a loose-type panicle. In rice, the *lax* mutant exhibits an opposite pattern in which vegetative branching is normal, but the axillary meristems are severely blocked in the reproductive stage. In YUM111 mutant rice, vegetative growth and development were normal, but after phase transition, inflorescence development was distorted, and lateral panicle branches were barely formed, resulting in fewer spikelets (figure 1).

The mutant phenotype was evident from early inflorescence development, where loosely arranged panicle branches were observed in the mutant, while the wild type showed a compact arrangement (figure 2a). Occasionally, primary and secondary rachis branches could not develop from panicle node and primary rachis nodes, respectively, in the mutant

Table 1. Important agronomic traits of wild type and mutant in rice.

Plant ID	Type	DH	CL	LL	LW	TN	PL	PN	SN	SF	GW	PRB	SRB	RN	RIL
YUC005	Wt	75±4*	69.2±1.5	56.9±0.8	1.76±.05	25±5	24.4±.6	21±1	123±4**	95.5±0.5	2.45 ±.15	12±3*	7±3**	10±4**	2.9±0.4
YUM111	M	90±3	61.8±0.8	50.4±1.3	1.1±.06	19±4	18.5±.8	15±2	32±6	87.4±2	3.11±.08	9±3	2±1	5±3	6.5±0.5**

Wt, wild-type cultivar (Donghechal); M, mutant; DH, days to heading (defined as duration from transplantation to emergence of the first panicle); CL, culm length in centimeter (cm); LL, leaf length in cm; LW, leaf width in cm; TN, number of reproductive tiller per plant; PL, panicle length in cm; PN, panicle number per plant; SN, spikelet number per panicle; SF, spikelet fertility percentage; GW, 100-grain weight in gram; PRB, number of primary rachis branches; SRB, number of secondary rachis branches; RN, number of rachis nodes; RIL, rachis internode length in cm. Number of PRB per panicle and number of nodes per PRB from first five branches and number of SRB per PRB from first five branches were evaluated. Average number of SP per panicle were calculated from 15 panicles. SE, standard error. N=15 observation for each trait. Asterisks indicate statistically significant differences of mutant compared to Wt (* $P > 0.05$, ** $P < 0.01$).

(figure 2b). Moreover, initiation of lateral spikelets primordia was suppressed at the secondary rachis nodes, which failed to develop lateral spikelets. Furthermore, only the terminal node formed spikelets as terminal florets in the mutant, resulting in sparsely distributed and reduced seeds per panicle (figures 2a, b). The rachis internodes as well as primary and secondary rachis internodes were excessively elongated in the mutant, approximately two times longer than the wild type (figure 2c). On the other hand, the mutant had fewer rachis nodes, primary rachis branches, nodes per primary rachis branch, and secondary rachis branches per primary rachis branch than the wild type (figure 2d).

The *lax* mutations include the *lax1* and *lax2* alleles (Futsuhara *et al.* 1979; Tabuchi *et al.* 2011; Dai *et al.* 2022), where the proliferation of meristem cells begins but fails to form axillary meristems (Oikawa and Kyozuka 2009), and the significant reduction of primary and secondary branches was consistent with the present *lax* mutation (Komatsu *et al.* 2001, 2003; Matin and Kang 2012; Lv *et al.* 2023). Moreover, the YUM111 mutant is consistent with previous reports of mutations in the *lax1-6* allele, which was confirmed to be a deletion mutant of the helix–loop–helix transcription factor, resulting in lack of lateral branch development and spikelet formation (Matin and Kang 2012).

In most of the *lax* and similar panicle mutants, including *lax1*, *lax2*, *lax1-1*, *LAX2-4*, and *branch one seed 1-1* (*bos1-1*), vegetative branching was normal, but axillary meristem formation was severely suppressed in the reproductive development stage. In addition, the panicle branches failed to develop completely, and only a terminal spikelet was formed, having no lateral spikelet (Futsuhara *et al.* 1979; Komatsu *et al.* 2001, 2003; Tabuchi *et al.* 2011; Dai *et al.* 2022; Lv *et al.* 2023). All reports show that the final yield was reduced dramatically in *lax* mutations (Li *et al.* 2021; Dai *et al.* 2022; Lv *et al.* 2023).

Other agronomic traits of the mutant plant

In addition to the mutant phenotypes, several important morpho-physiological traits were also observed and compared with the wild-type (normal) plants using the standard evaluation system described by the IRRI. Most traits, including the number of effective tillers and panicles (TN), plant height, and 1000-grain weight (GW), were similar in the mutant plants to those of the wild-type plants. On the other hand, the days to flowering (DH) and the grain number per panicle (SN) were reduced significantly in the mutant than in the wild-type (table 1). These results were identical to the other panicle-associated mutants, which showed a lower seed-setting rate than the controls (Dai *et al.* 2022; Lv *et al.* 2023). The panicle morphology-related traits also showed significant differences. The numbers of rachis nodes (RN) and rachis branches (PBR and SBR) were significantly lower, and the rachis internodes (RIL) were elongated in the

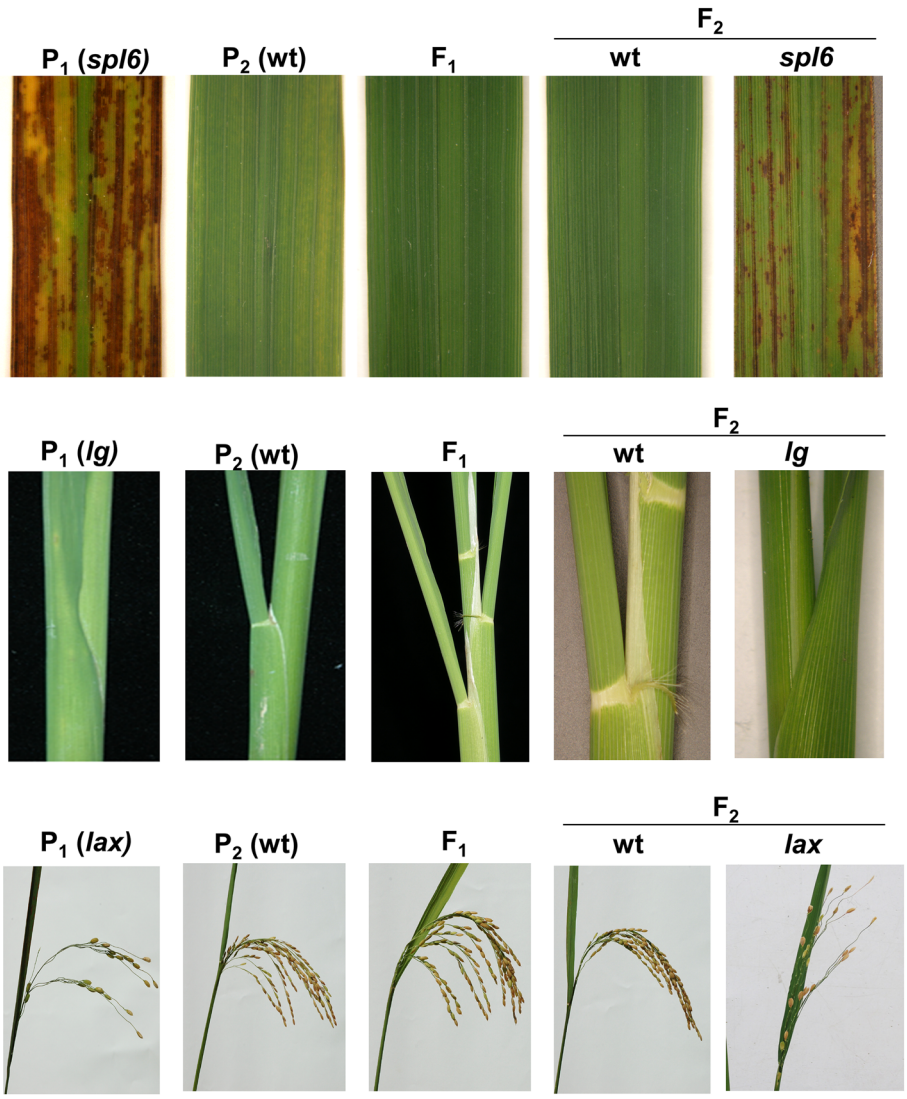

Figure 3. Representative of the phenotypic segregation at the F_2 generation of the *spl6*, *lg*, and *lax* genes. Both parents (P_1 and P_2), cross-driven F_1, and representatives of the F_2 phenotypes of plants for the three genes of concern are shown.

mutant compared to the wild type. In particular, only terminal spikelets formed in the mutant, which had no lateral spikelets. Therefore, the average seed per panicle was reduced drastically in the mutant (table 1).

Inheritance pattern of the spl6, lg, and lax genes in the segregating generation

Reciprocal cross-pollination was performed between a mutant (YUM111) and two wild-type rice lines (IRRI347 and Donghaechal). All phenotypic features were documented from the F_1 and F_2 plants throughout their developmental stages. The derived F_1 plants did not form any lesions in the leaf until maturation. The leaf blade and leaf sheath junction point were clearly surrounded by a white collar, auricles, and ligules, indicating the wild-type phenotype for the *lg* character and a panicle structure similar to the wild-type plant (figures 3 and 4). Similar results were also obtained from reciprocal crosses of the parental combination. Hence, a recessive nuclear gene controlled these mutations. The phenotypic segregation of individual mutations was further investigated in F_2 generation. The concerned genes were segregated into wild and mutant types (figure 3). The wild type to mutant ratio was then calculated to determine if they fit the Mendelian segregation ratio of 3:1.

For the segregation of the *spl6* gene at a 3:1 ratio, the calculated chi-square (χ^2) values of reciprocal crosses ($\chi^2_{3:1}$ =0.533 and 1.36, P=0.45 and 0.25, df=1) (table 2) proved this fitness as the values were less than the tabulated χ^2 value ($\chi^2_{3:1}$ =3.84). Five hundred and fifty-eight F_3 plants derived from selfing of one of the dominant F_2 plants (SGK05010-

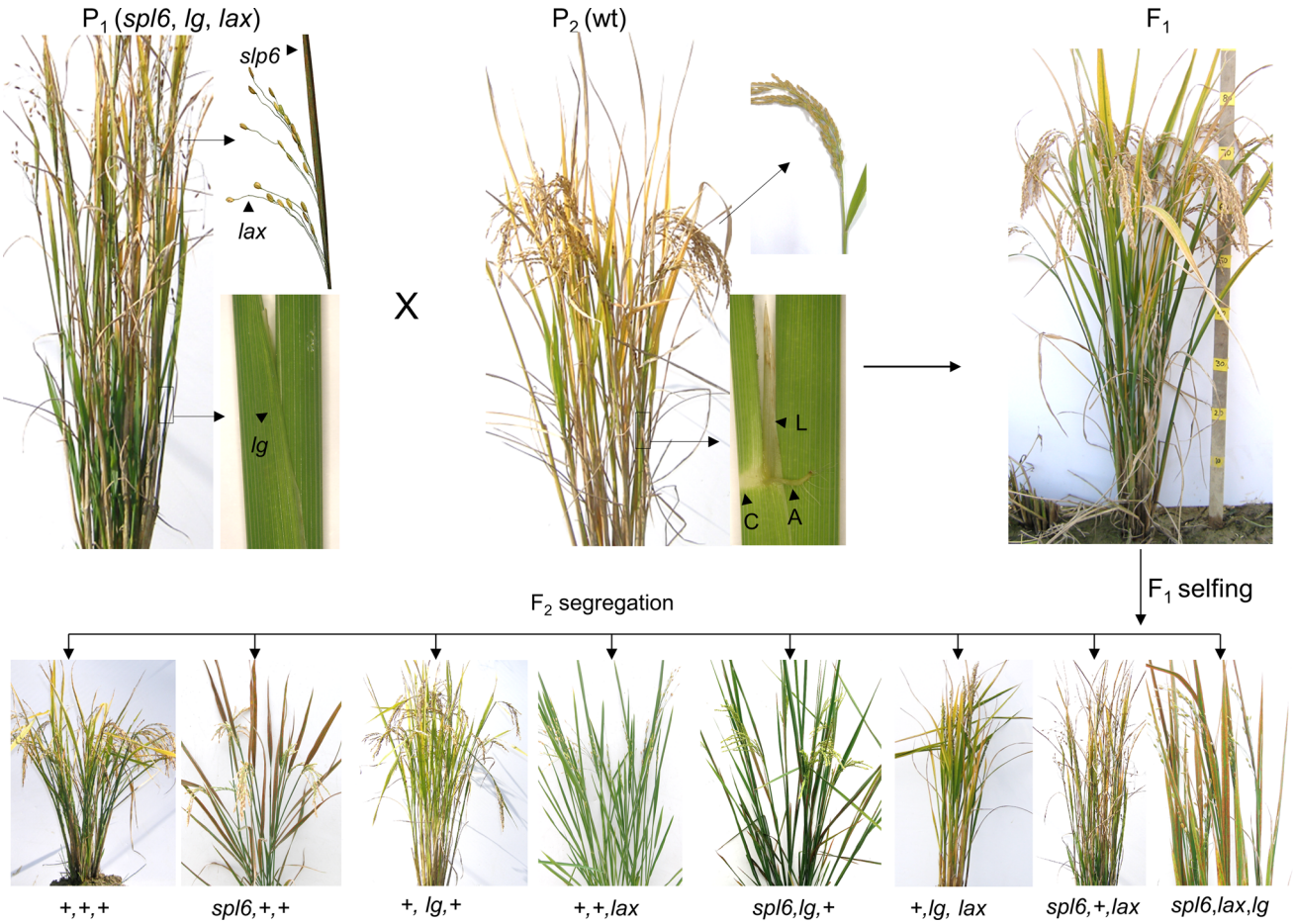

Figure 4. Phenotype of matured parental plants and their offspring at different generations. P_1, mutant parent as pollen receptor (YUM111); P_2, wild type parents as Indica type pollen donor (IRRI347) with a magnification of the mutant parts; F_1, hybrid generation of a cross between P_1 and P_2; F_2, representative phenotypes of the segregation populations developed from F_1 selfing, where +, +, + is normal for all characters; *spl6*, +, + denotes the mutant for spl character and normal for other character; +, *lg*, + is the mutant for the *lg* character and normal for the other; +, + is the *lax* mutant for lax character and normal for other, and similar for the other.

Table 2. Segregation of the *spl6* gene at the F_2 and F_3 generations from reciprocal crosses.

				Segregation in F_2				
ID	Cross combination	Gene concerned	F_1 phenotype	Wt	Mutant	Total	χ^2 (3:1)	*P*-value
SGK05010	YUM111 ♂ × IRRI347 ♀	*spl6*	Wt	124	36	160	0.533	0.45
SGK05011	IRRI347 ♂ × YUM111♀	*spl6*	Wt	161	44	205	1.36	0.25
				Segregation in F_3				
ID	Cross combination	Gene concerned	F_2 phenotype	Wt	Mutant	Total	χ^2 (3:1)	*P*-value
SGK05010-71	F_2 self-pollination	*spl6*	Wt (heterozygous)	425	133	558	0.405	0.55

71) segregated at 425 (wild type) to 133 (*spl6*), which also fited the Mendelian 3:1 ratio with a χ^2 value of 0.405 (*P*=0.55, df=1), indicating the heterozygosity of the SGK05010-71 plant (table 2).

Similarly, among the 124 dominant plants evaluated (table 2), 49 were homozygous dominant (no segregation), and the other 75 were heterozygous (segregated at 54:21=3:1). On the other hand, all 36 *spl6* mutant plants produced only mutant progeny, indicating their recessive homozygosity. Finally, the genotypes of all of the F_2 plants were also calculated to fit the Mendelian genotype segregation ratio of 1:2:1 (+/+: +/

Table 3. Genotypic segregation ratios of the *spl6* gene in the F_2 populations obtained from F_3 phenotypes.

	Segregation number					
Cross	+/+	+/*spl6*	*spl6*/*spl6*	Total	χ2 (1:2:1)	*P*-value
spl6/IRRI347	49	75	36	160	2.71	0.25

+/+; homozygous dominant, +/*spl6*; heterozygous, *spl6*/*spl6*; homozygous recessive.

Table 4. Segregation of the *lg* gene at the F_2 and F_3 generations from reciprocal crosses.

				Segregation in F_2				
ID	Cross combination	Gene concerned	F_1 phenotype	Wt	Mutant	Total	χ^2 (3:1)	*P*-value
SGK05010	YUM111 ♂ × IRRI347 ♀	*lg*	Wt	135	40	175	0.428	0.50
SGK05011	IRRI347 ♂ × YUM111♀	*lg*	Wt	156	41	197	1.84	0.15
				Segregation in F_3				
ID	Cross combination	Gene concerned	F_2 phenotype	Wt	Mutant	Total	χ^2 (3:1)	*P*-value
SGK05010-71	F_2 self-pollination	*lg*	Wt (heterozygous)	430	134	564	0.464	0.50

Table 5. Segregation of the *lax* gene at the F_2 and F_3 generations from reciprocal crosses.

				Segregation in F_2				
ID	Cross combination	Gene concerned	F_1 phenotype	Wt	Mutant	Total	χ^2 (3:1)	*P*-value
SGK05010	YUM111 ♂ × IRRI347 ♀	*lax*	Wt	79	19	98	1.64	0.20
SGK05011	IRRI347 ♂ × YUM111♀	*lax*	Wt	119	28	147	2.77	0.10
				Segregation in F_3				
ID	Cross combination	Gene concerned	F_2 phenotype	Wt	Mutant	Total	χ^2 (3:1)	*P*-value
SGK05010-71	F_2 self-pollination	*lax*	Wt (heterozygous)	412	152	564	1.14	0.30

spl6: *slp6*/*spl6*) with a χ^2 value of 2.71 (P=0.25, df=2) (table 3).

In case of *lg* gene, the χ^2 (3:1) values of segregation data from the reciprocal crosses (χ^2 =0.428 and 1.84, P=0.50 and 0.15, df=1) (table 4) proved this fitness because the values were less than the tabulated χ^2 value. The heterozygosity of the SGK05010-71 plant for the *lg* mutant was confirmed from the χ^2 value of 0.464 (P=0.50, df=1) (table 4).

In the case of the *lax* gene, the χ^2 (3:1) results of the segregation data (1.64 and 2.77) also proved this fitness (P=0.20 and 0.10, df=1) (table 5). The heterozygosity of the SGK05010-71 plant for the *lax* mutant was confirmed from the χ^2 value of 1.14 (P=0.30, df=1) (table 5). Overall, the *spl6*, *lg*, and *lax* phenotypes in rice are genetically stable and controlled by a single recessive nuclear gene.

Majority of the identified rice spotted leaf mutants are regulated by recessive genes (Takahashi *et al.* 1999; Yin *et al.* 2000; Balagué *et al.* 2003; Liu *et al.* 2004; Zeng *et al.* 2004; Kang *et al.* 2021; Yuchun *et al.* 2021; Yan *et al.* 2022). On the other hand, with some exceptions, *Spl7*, *Spl18*, and *Spl36* are dominant (Yamanouchi *et al.* 2002; Mori *et al.* 2007; Cai *et al.* 2021). In wheat, the *TaSpl1* of the spotted leaf mutant is controlled by a dominant gene, which was repressed by two other dominant genes, *TaSpl1-I1* and *TaSpl1-I2* (Zhang *et al.* 2021).

The *lg* and *lax* mutations are also controlled by a single recessive gene. The *lg* gene has been reported to be recessive located on rice chromosome 4 (Nagao and Takahashi 1963; Lee *et al.* 2007b;). Rice liguleless mutant, *Oslg1-3* was inherited as a single recessive gene model, and the corresponding gene *OsLG1* was localized to rice chromosome 4 (Morinaga 1938; Maekawa *et al.* 1981; Xu *et al.* 2010). Becraft *et al.* (1990) reported one of the important discoveries in plant morphology and development. They found

that, the maize *liguleless-1* gene affects ligule development and is controlled by a recessive mutation. Further studies reported that single recessive genes also control maize liguleless genes *lg2* and *lg3* (Harper and Freeling 1996; Muehlbauer *et al.* 1997). Furthermore, some dominant *Lg* mutations have also been identified in maize (Fowler and Freeling 1996). On the other hand, most of the rice *lax* alleles are recessive and identified on chromosome 1 (Kinoshita 1995; Nagato and Yoshimura 1998; Komatsu *et al.* 2001, 2003; Matin and Kang 2012). By contrast, the rice *lax2* and *lax2-4* mutations were mapped on chromosome 4 controlled by a single nuclear recessive gene, Os04g0396500 (Tabuchi *et al.* 2011) and LOC_Os04g32510 (Dai *et al.* 2022), respectively. The maize *lax* gene has also been identified as recessive (McSteen *et al.* 2000).

Linkage analysis among spl6, lg, and lax genes

The YUM111 genotype exhibited *spl6*, *lg*, and *lax* gene mutations, and the F_1 plants had normal phenotypes similar to the wild-type parent regarding all three mutations, indicating the recessive nature of each gene. When considering the co-segregation of *spl6* and *lg* genes, they segregate independently and fit the Mendelian 9:3:3:1 ratio. The χ^2 result of the segregation data (χ^2=6.19, *P*=0.10, df=3) (table 6) proved this fitness because the value was less than the χ^2 table value ($\chi^2_{9:3:3:1}$ =7.815).

The co-segregation of the *lg* and *lax* genes also segregated independently of each other according to the Mendelian 9:3:3:1 ratio because the calculated χ^2 value (χ^2=6.35, *P*=0.08, df=3) (table 6) was less than the tabulated χ^2 value ($\chi^2_{9:3:3:1}$ =7.815). Hence, the *spl6* and *lg* genes; and the *lg* and *lax* genes are not linked.

On the other hand, co-segregation of *spl6* and *lax* genes did not follow the independent segregation pattern of the Mendelian 9:3:3:1 ratio. The calculated χ^2 value (χ^2=363.67 *P*>0.0001, df=3) was much higher than the tabulated value of χ^2 ($\chi^2_{9:3:3:1}$=7.815), which rejects the hypothesis of their independent segregation (table 6). Therefore, *spl6* and *lax* genes are linked to each other.

With three genes not linked to Mendelian genetics, each parent can produce eight different gametes. This produces 64 possible genotype combinations, and the phenotypic ratio of the trihybrid cross is 27:9:9:9:3:3:3:1, which is the visible trait of the offspring at the end of the trihybrid cross. In the current experiments, eight different phenotypic combinations of three genes were obtained in segregating generations. These include the wild type for all genes (+, +, +), the mutant for *spl6* and the other wild type (*spl6*, +, +), the mutant for *lg* and the other wild type (+, *lg*, +), the mutant for *lax* and the other wild type (+, +, *lax*), the mutant for *spl6* and *lg* (*spl6*, *lg*, +), the mutant for *lg* and *lax* (+, *lg*, *lax*), the mutant for *spl6* and *lax* (*spl6*, +, *lax*), and all three mutants (*spl6*, *lax*, *lg*) (figure 4). On the other hand, these phenotypic combinations were not in accordance with the Mendelian trihybrid segregation that also approved the linkage of at least any gene pair.

Crossing two plants with different genotypes will result in offspring with different genotypes compared to parents. Offspring with different genotypes from their parents are the recombinant type. The recombination percentages and their standard errors are calculated if a significant deviation is detected. A significant deviation was detected for *spl6* and *lax* segregations. Therefore, the recombination percentage between them was calculated. In the case of *spl6* and *lax* segregation, out of 548 segregating individuals, 372 were dominant, and 124 were recessive parental types, whereas 20

Table 6. Co-segregation of the *spl6* and *lg*, *spl6* and *lax*, and *lg* and *lax* genes at the F_3 generations from dihybrid cross.

ID	Cross combination	Gene combination	F_1 phenotype	Segregation					χ^2 (9:3:3:1)	*P*-value
				+, +	+, *spl6*	+, *lg*	*spl6, lg*	Total		
SGK05010	YUM111♂ × IRRI347♀ (*spl6*,*lax*,*lg*) × (+,+,+)	*spl6, lg*	Wt	324	94	87	43	548	6.19	0.10
				+, +	+, *spl6*	+, *lax*	*spl6, lax*	Total		
SGK05010	YUM111♂ × IRRI347♀ (*spl6*,*lax*,*lg*) × (+,+,+)	*spl6, lax*	Wt	372	20	32	124	548	363.67	>0.0001
				+, +	+, *lg*	+, *lax*	*lg, lax*	Total		
SGK05010	YUM111♂ × IRRI347♀ (*spl6*,*lax*,*lg*) × (+,+,+)	*lg*, *lax*	Wt	306	86	112	44	548	6.35	0.08

SGK05010, lab cross ID; *spl6*, Japonica type rice cultivar (YUM111); IRRI347, Indica type rice cultivar; SGK05010-71, one of the heterozygous plants confirmed after F_3 segregation; Wt, wild type; (+, +) normal for both characters; (+, *spl6*) normal for liguleless character and mutant for spl character; (+, *lg*) normal for spl character and mutant for *lg* character; (*spl6*, *lg*) mutant for both characters, and similar fashion for other also.

and 32 plants were the recombinant type, indicating 90.51% are the parental classes, and 9.48% are the recombinant classes (table 6). Hence, the two genes are linked because the number of parent classes was greater than the recombinant class. The linkage between *spl6* and *lax* was estimated to be in the repulsion phase from the calculated recombination percentages because of excess of *lax* plants in F_2 populations. Therefore, the frequency of a single cross-over between them was calculated to be ∼9.4%, indicating *spl6* and *lax* might be 9.4 cM apart from each other.

Construction of linkage maps is essential for genetics, molecular research, and breeding programmes, especially for genotypes with multiple mutation phenotypes. Here, the *lg* gene was segregated independently with *spl6* and *lax* at 9:3:3:1, indicating that they are not linked individually. On the other hand, the *lax* gene did not follow the 9:3:3:1 ratio but was co-segregated with *spl6*, indicating that they are linked in chromosome 1. In addition, in this study, *lax* and *spl6* were located 9.4 cM away from each other. In the rice physical map, *lax* is located at the 121.1 cM locus, and *spl6* is located at the 126.6 cM locus (figure 5) (Kishimoto *et al.* 1992; Kinoshita, 1995; Yoshimura *et al.* 1997).

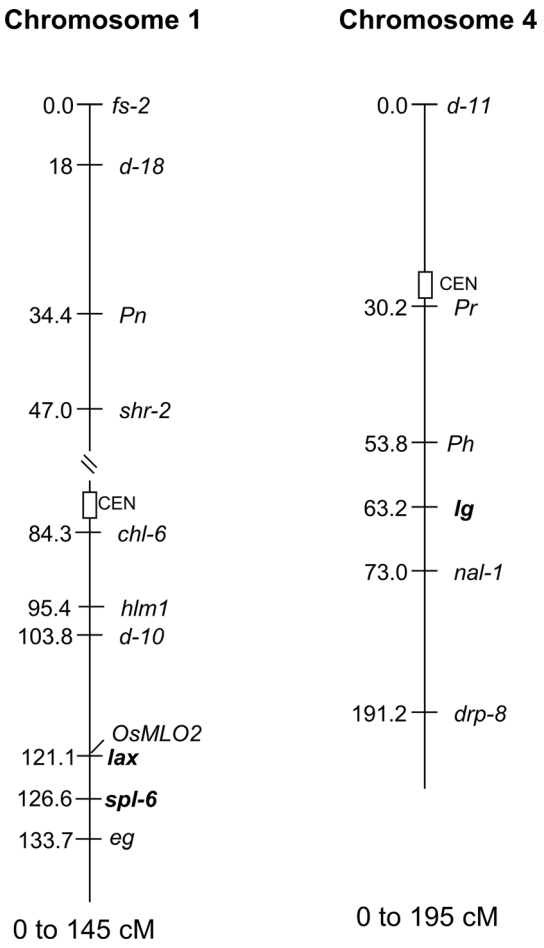

Figure 5. Linkage map of the rice chromosomes. The genes and their corresponding location in cM are demonstrated for chromosomes 1 and 4. Modified from Yoshimura *et al.* (1997).

Conclusion

Phenotypic mutations are an excellent source for exploring the genetic mechanisms responsible for specific mutations and accurately detecting mutation points. Therefore, the mutant genotype containing three mutations, *spl6*, *lax*, and *lg*, provides the opportunity to reveal multiple mechanisms and common effects in a single experiment. LMMs are ideal for studying disease resistance and PCD in plants to improve crop yields. Therefore, *spl6* LMM provides a valuable tool to reveal the molecular mechanisms determining PCD in rice. The *lg* and *lax* genes can describe the plant morphology and architecture. These two genes have tillering and panicle branching as important agronomic traits associated with the rice grain yield. Therefore, identifying *lg* and *lax* genes and elucidating their molecular mechanisms will be useful for rice production management and genetic improvement. The phenotype of each mutation in these materials was studied intensively. The results showed that they are controlled in a recessive manner. Therefore, understanding *lax* genes, which determine the rachis length, branching, rachis node density, and inter-rachis length of spikelet development, may contribute to breeding for higher yielding rice.

Author contributions

MNM: conceptualization, methodology, data curation, formal analysis, original draft preparation and writing. KEL: methodology and editing. SGK: conceptualization, investigation, resources, visualization, supervision, writing and editing. All authors have read and agreed for the publication of the article.

References

Balagué C., Lin B., Alcon C., Flottes G., Malmström S., Köhler C. *et al.* 2003 HLM1, an essential signaling component in the hypersensitive response, is a member of the cyclic nucleotide-gated channel ion channel family. *Plant Cell* **15**, 365–379.

Becraft P. W., Bongard-Pierce D. K., Sylvester A. W., Poethig R. S. and Freeling M. 1990 The *liguleless-1* gene acts tissue specifically in maize leaf development. *Dev. Biol.* **141**, 220–232.

Bell A. D., Bryan A. 2008 *Plant form: an illustrated guide to flowering plant morphology.* Oxford University Press, Oxford.

Bruggeman Q., Raynaud C., Benhamed M. and Delarue M. 2015 To die or not to die? Lessons from lesion mimic mutants. *Front. Plant Sci.* **6**, 24.

Cai L., Yan M., Yun H., Tan J., Du D., Sun H. *et al.* 2021 Identification and fine mapping of lesion mimic mutant spl36 in rice (*Oryza sativa* L.). *Breed. Sci.* **71**, 510–519.

Chen Z., Yin W., Li X., Lu T., Ye H., Dai G. *et al.* 2022 OsSPL88 Encodes a cullin protein that regulates rice growth and development. *Front. Genet.* **13**, 918973.

Dai D., Chen J., Du C., Liang M., Wu M., Mou T. *et al.* 2022 A 2-MB chromosome inversion interrupted transcription of *lax2-4* and generated pleiotropic phenotypes in rice. *J. Plant Growth Regul.* **41**, 2328–2337.

Fowler J. E. and Freeling M. 1996 Genetic analysis of mutations that alter cell fates in maize leaves: dominant Liguleless mutations. *Dev. Genet.* **18**, 198–222.

Futsuhara Y., Kondo S., Kitano H. and Mii M. 1979 Genetical studies on dense and lax panicles in rice: I. Character expression and mode of lax panicle rice. *Jpn. J. Breed.* **29**, 151–158.

Harper L. and Freeling M. 1996 Interactions of *liguleless1* and *liguleless2* function during ligule induction in maize. *Genetics* **144**, 1871–1882.

Hoshikawa K. 1989 *The growing rice plant. An anatomical monograph*, pp. 199–205. Nosan Gyoson Bunka kyokai, Tokyo.

Jiang R., Zhou S., Da X., Chen T., Xu J., Yan P. and Mo X. 2022 Ubiquitin-specific protease 2 (OsUBP2) negatively regulates cell death and disease resistance in rice. *Plants* **11**, 2568.

Kang S. G., Matin M. N., Bae H. and Natarajan S. 2007 Proteome analysis and characterization of phenotypes of lesion mimic mutant *spotted leaf 6* in rice. *Proteomics* **7**, 2447–2458.

Kang S. G., Lee K. E., Singh M., Kumar P. and Matin M. N. 2021 Rice lesion mimic mutants (LMM): The current understanding of genetic mutations in the failure of ROS scavenging during lesion formation. *Plants* **10**, 1598.

Kinoshita T. 1995 Report of committee on gene symbolization, nomenclature and linkage groups. *Rice Genet. Newslett.* **12**, 9–154.

Kishimoto N., Shimosaka E., Matsuura S. and Saito A. 1992 A current RFLP linkage map of rice: Alignment of the molecular map with the classical map. *Rice Genet. Newslett.* **9**, 118–124.

Komatsu M., Maekawa M., Shimamoto K. and Kyozuka J. 2001 The LAX1 and FRIZZY PANICLE 2 genes determine the inflorescence architecture of rice by controlling rachis-branch and spikelet development. *Dev. Biol.* **231**, 364–373.

Komatsu M., Chujo A., Nagato Y., Shimamoto K. and Kyozuka J. 2003 FRIZZY PANICLE is required to prevent the formation of axillary meristems and to establish floral meristem identity in rice spikelets. *Development* **130**, 3841–4385.

Kumamaru T., Satoh H., Iwata N., Omura T., Ogawa M. and Tanaka K. 1988 Mutants for rice storage proteins: 1. Screening of mutants for rice storage proteins of protein bodies in the starchy endosperm. *Theor. Appl. Genet.* **76**, 11–16.

Lee D.-Y., Lee J., Moon S., Park S. Y. and An G. 2007a The rice heterochronic gene *SUPERNUMERARY BRACT* regulates the transition from spikelet meristem to floral meristem. *Plant J.* **49**, 64–78.

Lee J., Park J.-J., Kim S. L., Yim J. and An G. 2007b Mutations in the rice liguleless gene result in a complete loss of the auricle, ligule, and laminar joint. *Plant Mol. Biol.* **65**, 487–499.

Li G., Zhang H., Li J., Zhang Z. and Li Z. 2021 Genetic control of panicle architecture in rice. *Crop J.* **9**, 590–597.

Li C., Liu H., Wang J., Pan Q., Wang Y., Wu K. *et al*. 2022 Characterization and fine mapping of a lesion mimic mutant (*Lm5*) with enhanced stripe rust and powdery mildew resistance in bread wheat (*Triticum aestivum* L.). *Theor. Appl. Genet.* **135**, 421–438.

Liu G., Wang L., Zhou Z., Leung H., Wang G. L. and He C. 2004 Physical mapping of a rice lesion mimic gene, Spl1, to a 70-kb segment of rice chromosome 12. *Mol. Genet. Genomics* **272**, 108–115.

Liu K., Cao J., Yu K., Liu X., Gao Y., Chen Q. *et al*. 2019 Wheat *TaSPL8* modulates leaf angle through auxin and brassinosteroid signaling. *Plant Physiol.* **181**, 179–194.

Liu R., Lu J., Zheng S., Du M., Zhang C., Wang M. *et al*. 2021 Molecular mapping of a novel lesion mimic gene (*lm4*) associated with enhanced resistance to stripe rust in bread wheat. *BMC Genomic Data* **22**, 1–9.

Lv Y., Zhang X., Hu Y., Liu S., Yin Y. and Wang X. 2023 BOS1 is a basic helix–loop–helix transcription factor involved in regulating panicle development in rice. *Front. Plant Sci.* **14**, 1162828.

Ma J., Wang Y., Ma X., Meng L., Jing R., Wang F. *et al*. 2019 Disruption of gene SPL 35, encoding a novel CUE domain-containing protein, leads to cell death and enhanced disease response in rice. *Plant Biotechnol. J.* **17**, 1679–1693.

Maekawa M. 1988 A new allele at the lg locus conferring short ligule. *Rice Genet. Newslett.* **5**, 87–89.

Maekawa M., Kinoshita T. and Takahashi M. 1981 A new gametophyte gene in the second linkage group of rice: genetical studies on rice plant. *LXXVI. J. Fac. Agric. Hokkaido Univ.* **60**, 107–114.

Matin M. N. and Kang S. G. 2012 Genetic and phenotypic analysis of *lax1-6*, a mutant allele of *LAX PANICLE1* in rice. *J. Plant Biol.* **55**, 50–63.

Matin M. N., Suh H. S. and Kang S. G. 2006 Characterization of phenotypes of rice lesion resembling disease mutants. *Korean J. Genet.* **28**, 221–228.

McSteen P., Laudencia-Chingcuanco D. and Colasanti J. 2000 A floret by any other name: control of meristem identity in maize. *Trend. Plant Sci.* **5**, 61–66.

Mori K., Kinoshita T. and Takahashi M. 1973 Linkage relationships of genes for some mutant characters of rice kept in Kyushu University-Genetical studies on rice plant. *LV. Mem. Fac. Agr. Hokkaido Univ.* **8**, 377–385.

Mori M., Tomita C., Sugimoto K., Hasegawa M., Hayashi N., Dubouzet J. G. *et al*. 2007 Isolation and molecular characterization of a *Spotted leaf 18* mutant by modified activation-tagging in rice. *Plant Mol. Biol.* **63**, 847–860.

Morinaga T. 1938 Inheritance in rice, *Oryza sativa* L., II. Linkage between the gene for purple plant color and the gene for liguleless. *Jpn. J. Bot.* **9**, 121–129.

Muehlbauer G. J., Fowler J. E. and Freeling M. 1997 Sectors expressing the homeobox gene *liguleless3* implicate a time-dependent mechanism for cell fate acquisition along the proximal-distal axis of the maize leaf. *Development* **124**, 5097–5106.

Nagao S. and Takahashi M. 1963 Trial Construction of Twelve Linkage Groups in Japanese Rice:(Genetical Studies on Rice Plant, XXVII). *J. Fac. Agric. Hokkaido Univ.* **53**, 72–130.

Nagato Y. and Yoshimura A. 1998 Report of the committee on gene symbolization, nomenclature and linkage map. *Rice Genet. Newslett.* **15**, 13–74.

Oikawa T. and Kyozuka J. 2009 Two-step regulation of *LAX PANICLE1* protein accumulation in axillary meristem formation in rice. *Plant Cell* **21**, 1095–1108.

Qin L., Wu X. and Zhao H. 2023 Molecular and functional dissection of LIGULELESS1 (LG1) in plants. *Front. Plant Sci.* **14**, 1190004.

Qiu Z., Zhu L., He L., Chen D., Zeng D., Chen G. *et al*. 2019 DNA damage and reactive oxygen species cause cell death in the rice local lesions 1 mutant under high light and high temperature. *New Phytol.* **222**, 349–365.

Ruan B., Hua Z., Zhao J., Zhang B., Ren D., Liu C. *et al*. 2019 *Os ACL-A2* negatively regulates cell death and disease resistance in rice. *Plant Biotech. J.* **17**, 1344–1356.

Sanchez A. C. 1998 A gene for collarless phenotype in rice. *Rice Genet. Newslett.* **15**, 99.

Shang H., Li P., Zhang X., Xu X., Gong J., Yang S. *et al*. 2022 The Gain-of-function mutation, *OsSpl26*, positively regulates plant immunity in rice. *Int. J. Mol. Sci.* **23**, 14168.

Tabuchi H., Zhang Y., Hattori S., Omae M., Shimizu-Sato S., Oikawa T. *et al*. 2011 *LAX PANICLE2* of rice encodes a novel nuclear protein and regulates the formation of axillary meristems. *Plant Cell* **23**, 3276–3287.

Takahashi A., Kawasaki T., Henmi K., Shii K., Kodama O., Satoh H. and Shimamoto K. 1999 Lesion mimic mutants of rice with alterations in early signaling events of defense. *Plant J.* **17**, 535–545.

Tian J., Wang C., Xia J., Wu L., Xu G., Wu W. *et al*. 2019 Teosinte ligule allele narrows plant architecture and enhances high-density maize yields. *Science* **365**, 658–664.

Wang L., Pei Z., Tian Y. and He C. 2005 *OsLSD1*, a rice zinc finger protein, regulates programmed cell death and callus differentiation. *Mol. Plant-Microbe Interact.* **18**, 375–384.

Wang L., Wen R., Wang J., Xiang D., Wang Q., Zang Y. *et al*. 2019 Arabidopsis UBC 13 differentially regulates two programmed cell death pathways in responses to pathogen and low-temperature stress. *New Phytol.* **221**, 919–934.

Wang B., Lin Z., Li X., Zhao Y., Zhao B., Wu G. *et al*. 2020 Genome-wide selection and genetic improvement during modern maize breeding. *Nat. Genet.* **52**, 565–571.

Wang R., Liu C., Chen Z., Sun S. and Wang X. 2021 *Oryza sativa LIGULELESS 2s* determine lamina joint positioning and differentiation by inhibiting auxin signaling. *New Phytol.* **229**, 1832–1839.

Williams B. and Dickman M. 2008 Plant programmed cell death: can't live with it; can't live without it. *Mol. Plant Pathol.* **9**, 531–544.

Wu H., Dai G., Yuchun R., Wu K., Wang J., Hu P. *et al*. 2023 Disruption of *LEAF LESION MIMIC 4* affects ABA synthesis and ROS accumulation in rice. *Crop J.* **11**, 1341–1352.

Xia S., Cui Y., Li F., Tan J., Xie Y., Sang X. and Ling Y. 2019 Phenotypic characterizing and gene mapping of a lesion mimic and *premature senescence 1* (*lmps1*) mutant in rice (*Oryza sativa* L.). *Acta Agron. Sin.* **45**, 46–54.

Xu Y., Deng M., Wu X., Bao L., Cheng J., Jing W. *et al*. 2010 Cloning and application of a rice liguleless gene. *J. Nuclear Agric. Sci.* **24**, 436–441.

Yamagishi J., Miyamoto N., Hirotsu S., Laza R. C. and Nemoto K. 2004 QTLs for branching, floret formation, and pre-flowering floret abortion of rice panicle in a temperate japonica× tropical japonica cross. *Theor. Appl. Genet.* **109**, 1555–1561.

Yamanouchi U., Yano M., Lin H., Ashikari M. and Yamada K. 2002 A rice spotted leaf gene, *Spl7*, encodes a heat stress transcription factor protein. *Proc. Natl. Acad. Sci. USA* **99**, 7530–7535.

Yan J., Fang Y. and Xue D. 2022 Advances in the genetic basis and molecular mechanism of lesion mimic formation in rice. *Plants* **11**, 2169.

Yao Y., Zhou J., Cheng C., Niu F., Zhang A., Sun B. *et al*. 2022 A conserved clathrin-coated vesicle component, OsSCYL2, regulates plant innate immunity in rice. *Plant Cell Environ.* **45**, 542–555.

Yin Z., Chen J., Zeng L., Goh M., Leung H., Khush G. S. and Wang G.-L. 2000 Characterizing rice lesion mimic mutants and identifying a mutant with broad-spectrum resistance to rice blast and bacterial blight. *Mol. Plant-Microbe Interact.* **13**, 869–876.

Yoshida A., Ohmori Y., Kitano H., Taguchi-Shiobara F. and Hirano H. Y. 2012 *ABERRANT SPIKELET AND PANICLE1*, encoding a TOPLESS-related transcriptional co-repressor, is involved in the regulation of meristem fate in rice. *Plant J.* **70**, 327–339.

Yoshimura A., Ideta O. and Iwata N. 1997 Linkage map of phenotype and RFLP markers in rice. *Plant Mol. Biol.* **35**, 49–60.

Yuchun R. A. O., Ran J., Sheng W., Xianmei W. U., Hanfei Y. E., Chenyang P. A. N. *et al*. 2021 *SPL36* encodes a receptor-like protein kinase that regulates programmed cell death and defense responses in rice. *Rice* **14**, 1–14.

Zeng L.-R., Qu S., Bordeos A., Yang C., Baraoidan M., Yan H. *et al*. 2004 *Spotted leaf11*, a negative regulator of plant cell death and defense, encodes a U-box/armadillo repeat protein endowed with E3 ubiquitin ligase activity. *Plant Cell* **16**, 2795–2808.

Zhang Y., Liu Q., Zhang Y., Chen Y., Yu N., Cao Y. *et al*. 2019 LMM24 encodes receptor-like cytoplasmic kinase 109, which regulates cell death and defense responses in rice. *Intl. J. Mol. Sci.* **20**, 3243.

Zhang H., Xu X., Wang M., Wang H., Deng P., Zhang Y. *et al*. 2021 A dominant spotted leaf gene *TaSpl1* activates endocytosis and defense-related genes causing cell death in the absence of dominant inhibitors. *Plant Sci.* **310**, 110982.

Zhao M., Guo Y., Sun H., Dai J., Peng X., Wu X. *et al*. 2023 Lesion mimic mutant 8 balances disease resistance and growth in rice. *Front. Plant Sci.* **14**, 1189926.

Zheng Z., Hu H., Gao S., Zhou H., Luo W., Kage U. *et al*. 2022 Leaf thickness of barley: genetic dissection, candidate genes prediction and its relationship with yield-related traits. *Theor. Appl. Genet.* **135**, 1843–1854.

Ad-hoc editor: Hitendra Kumar Patel